

Adsorbate-induced surface reconstruction and surface-stress changes in Cu(100)/O: Experiment and theory

M. J. Harrison, D. P. Woodruff,* and J. Robinson

Physics Department, University of Warwick, Coventry CV4 7AL, United Kingdom

D. Sander, W. Pan,† and J. Kirschner

Max-Planck-Institut für Mikrostrukturphysik, Weinberg 2, D-06120 Halle, Germany

(Received 10 May 2006; revised manuscript received 11 July 2006; published 3 October 2006)

Using the crystal curvature technique we have measured the change in surface stress on Cu(100) induced by oxygen adsorption to produce, at 300 K, a $c(2 \times 2)$ overlayer phase, and at 500 K, the $(\sqrt{2} \times \sqrt{2})R45^\circ$ missing-row reconstructed phase. Density functional theory (DFT) slab calculations have also been performed of the absolute surface stress of the clean Cu(100) surface and these two chemisorbed oxygen phases. Both experiment and theory show that oxygen adsorption leads to a compressive change in the surface stress that is larger for the $c(2 \times 2)$ overlayer (experiment: -1.0 N/m; theory: -3.07 N/m) than for the missing-row reconstruction (experiment: -0.6 N/m; theory: -2.03 N/m). Furthermore, the DFT calculations show that the absolute compressive surface stress of the $c(2 \times 2)$ phase of -1.18 N/m is lowered by the reconstruction to an average value of -0.14 N/m. These results indicate that surface stress reduction plays a role in causing the reconstruction. The discrepancies between theory and experiment are discussed in the context of possible sources of error in both experiment and theory.

DOI: [10.1103/PhysRevB.74.165402](https://doi.org/10.1103/PhysRevB.74.165402)

PACS number(s): 68.35.Gy, 68.43.Bc

I. INTRODUCTION

While in many cases adsorption on surfaces leads to only minor modification of the outermost atomic layers of the substrate, typically in the form of local changes in interlayer spacings, there is also an important class of systems in which adsorption induces a reconstruction of the substrate surface, causing either significant changes in the atomic density of the outermost layer, or lateral distortions of the outermost one, or more layers (e.g., Ref. 1). It is implicit that such adsorbate-induced reconstruction is driven by a lowering of the total free energy, and *ab initio* total energy calculations are now performed routinely in surface science to assist in the determination of surface structures as well as in elucidating surface chemical reactions mechanisms. Total energy calculations alone, however, give no insight into the physical mechanisms that underlie surface reconstruction and contribute to the energy lowering. One such mechanism is the associated change in the surface stress (e.g., Ref. 2), and not only can this quantity be measured experimentally, but it is also rather straightforward to extract theoretical values of this quantity from total energy calculations (e.g., Ref. 3). Comparisons of these stress changes in specific systems provide a way of evaluating the general importance of this mechanism in influencing surface reconstruction.

Here we present the results of experimental measurements and *ab initio* theoretical calculations of the surface stress changes associated with one such adsorbate-induced surface reconstruction, namely the formation of a “missing-row” reconstruction on Cu(100) caused by the adsorption of atomic oxygen. Our results lead us to conclude that relief of surface stress does play a significant role in this reconstruction.

Based on theoretical calculations, it is generally accepted that clean metal surfaces are in a state of tensile surface stress. The lack of bonding partners for surface atoms in-

duces a redistribution of electronic valence charge near the surface. Typically this leads to some inward layer relaxation of the outermost atomic layer and to the tensile surface stress, both effects reflecting the general tendency towards a shorter bond length for atoms of reduced coordination. In cases in which this tensile surface stress of the ideally-terminated bulk structure is large enough, relaxation of the surface stress drives a reconstruction to a surface layer of higher atomic density and shorter interatomic distances, as in the well-known case of the “herring-bone” reconstruction of Au(111).²

On adsorbate-covered metal surfaces the influence of surface stress can be quite different. Many adsorbates on metal surfaces, especially electronegative species, lead to a surface stress change which is compressive, and in cases in which the absolute surface stress becomes compressive this may lead to an adsorbate-induced reconstruction to achieve longer interatomic distances within the surface. One specific case in which this is thought to occur^{2,4} is the adsorption of C onto Ni(100) in which the ordered 0.5 ML phase has a $(2 \times 2)p4g$ unit mesh, and an associated structure usually referred to as a “clock reconstruction,” in which there is an increase in the Ni-Ni spacing within the surface layer relative to the unreconstructed surface.⁵⁻⁷ N adsorption on Ni(100) leads to a similar $(2 \times 2)p4g$ clock reconstruction, but O adsorption at the same coverage of 0.5 ML leads to a simple $c(2 \times 2)$ surface unit mesh and no associated reconstruction.

By contrast, on Cu(100), 0.5 ML coverage of atomic oxygen leads to a quite different reconstruction involving ejection of every fourth $\langle 010 \rangle$ atomic row of surface layer Cu atoms, producing a $(\sqrt{2} \times 2\sqrt{2})R45^\circ$ unit mesh; the basic structural parameters of this phase appear to be well-established experimentally.⁸⁻¹² There have been a number of theoretical studies of this reconstruction in which different mechanisms have been discussed, generally in terms of elec-

tronic structure effects. Specifically, mechanisms suggested or identified (some of which overlap) include a Peierls instability or Jahn-Teller effect,¹³ the local bonding structure and resulting relative energy levels,¹⁴ the large dipole moment associated with a large effective charge on the adsorbed O atoms,¹⁵ and the role of long-range Coulomb interactions.¹⁶ Wuttig *et al.*¹³ have specifically ruled out surface stress as a possible driving force for the missing-row reconstruction, arguing that if surface stress relief played an important role in the Cu(100)/O system, one would expect to observe, instead, a clock reconstruction.¹³

However, our results suggest that this view might be too simplistic, as we find in both experiment and theory that the oxygen-induced compressive surface stress is lowered upon formation of the missing row reconstruction. Our study provides experimental and theoretical evidence that the removal of atomic rows, which is the characteristic of the missing row reconstruction, is a means to lower adsorbate-induced compressive surface stress. Whereas the $p4g$ reconstruction of Ni(100) is believed to lower compressive stress mainly due to the enlargement of all Ni-Ni interatomic distances within the surface, the missing row reconstruction on Cu(100) does so by reducing the atomic density in the surface layer, also allowing an increase in the Cu-Cu distances through local lateral relaxation adjacent to the missing rows.

II. EXPERIMENTAL DETAILS AND RESULTS

The oxygen-induced surface stress change was measured by the crystal curvature technique, described more fully elsewhere,¹⁷ in an ultrahigh vacuum chamber (UHV) with a base pressure below 1×10^{-10} mbar. A Cu(100) crystal (length along [010]: 13 mm, width: 3 mm, thickness: 0.127 mm) was clamped along its width at one end to a sample manipulator. Briefly, the adsorbate-induced surface stress change, $\Delta\tau$, leads to a change of curvature, $\Delta\kappa$, of the thin crystal, which was detected by an optical deflection technique. The surface stress change is then calculated from $\Delta\tau = \Delta\kappa Y t^2 / [6(1-\nu)]$. The radius of curvature is $R = 1/\kappa$, the Young modulus, Y , and the Poisson ratio, ν , of Cu are 66.7 GPa and 0.42, respectively, and the Cu sample thickness is given by t . The large length-to-width ratio >4 of the free part of the crystal, and the application of a two-beam curvature measurement, justifies the application of this simple relationship to extract quantitative stress values without any need for further corrections.¹⁷ The overall error bar for the derived stress values is estimated to be smaller than 10%. The curvature change is measured along the [010] direction. Due to the anisotropy of the missing row reconstruction, it is important to realize that both in-plane stress components [001] and [010] contribute to the curvature along [010].¹⁸ The LEED patterns of Fig. 1 indicate that the missing row reconstruction occurs with equal probability in two domains, rotated by 90° . Our result of the curvature measurement is therefore ascribed to the average surface stress change $\Delta\tau = 0.5(\Delta\tau_{\text{along missing row}} + \Delta\tau_{\text{perp. to missing row}})$.

The crystal was cleaned by cycles of ion bombardment (Ar^+ , 1 keV) and annealing at 720 K until no surface contamination could be detected by Auger electron spectroscopy

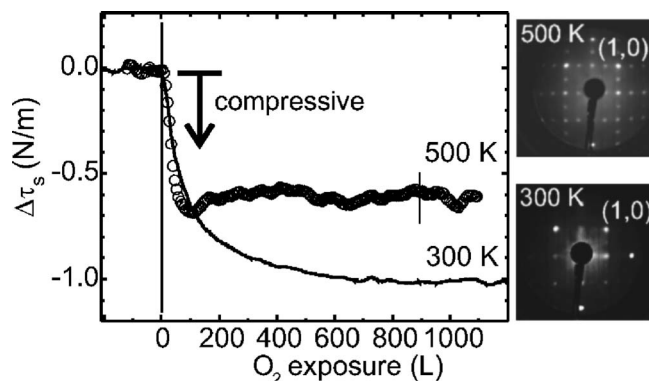


FIG. 1. Oxygen-induced compressive surface stress change of Cu(100) as measured during O_2 exposure at 300 K (solid line), and 500 K (open symbols), and resulting LEED patterns (images on the right). The vertical bars indicate the beginning and end of exposure at 500 K. The total exposure was 2000 L at 300 K, but no further stress change was observed beyond 1000 L. The resulting compressive surface stress change is -1 N/m at 300 K, but only -0.6 N/m at 500 K. The LEED patterns were recorded at 115 eV following these exposures. Exposure at 300 K leads to a $c(2 \times 2)$ pattern, whereas exposure at 500 K gives the missing row related $(\sqrt{2} \times 2\sqrt{2})R45^\circ$ pattern.

(surface contamination $<1\%$ of a monolayer), and sharp diffraction spots were observed by low-energy electron diffraction (LEED). The clean Cu(100) surface was exposed to oxygen, introduced into the UHV chamber with precision leak valves, at an O_2 partial pressure in the range $1-2 \times 10^{-6}$ mbar, as checked by an ion gauge and by a quadrupole mass spectrometer. The exposure is given in Langmuir units ($1 \text{ L} = 10^{-6}$ torr s). The back side of the crystal was not sputter-cleaned by Ar ion bombardment. We can therefore safely assume that the contamination renders the back side inert with respect to adsorption from the gas phase. This assumption is corroborated by our experimental finding that the same stress change was measured for a given gas exposure, independent of whether the dosing was achieved by changing the overall gas partial pressure in the UHV chamber, or by using a doser-tube facing the front side; this doser leads to a very significantly larger partial pressure at the front side of the sample than at the back side.¹⁸ All measured stress changes are therefore ascribed to stress changes of the front surface of the crystal.

To elucidate the role of surface stress for the oxygen-induced missing row reconstruction of Cu(100), measurements were made of the stress changes associated with the formation of both the unreconstructed $c(2 \times 2)\text{-O}$ and the missing row $(\sqrt{2} \times 2\sqrt{2})R45^\circ\text{-O}$ structures. The two structures were prepared by exposing Cu(100) to a few hundred L of oxygen at either 300 K or 500 K. Exposure at 300 K leads to the formation of the $c(2 \times 2)$ structure, while exposure at 500 K leads to the missing row $(\sqrt{2} \times 2\sqrt{2})R45^\circ$ structure for exposures in excess of 300 L, as characterized in earlier studies¹³ and confirmed by our own LEED observations.

Figure 1 summarizes the results of these measurements of the oxygen-induced surface stress changes of Cu(100), as measured at the surface temperatures of 300 K and 500 K.

TABLE I. Summary of calculated absolute surface stress on Cu(100) and for the two O adsorption structures, together with both calculated and experimental adsorbate-induced surface stress changes. In the case of the Cu(100)($\sqrt{2} \times 2\sqrt{2}$)R45°-O surface phase which has reduced twofold rotational symmetry the surface stress is anisotropic and two values are given for the calculations—the first value corresponds to the stress parallel to the missing rows of this reconstruction (the “ $\sqrt{2}$ ” direction, see Fig. 2) while the second value is the stress perpendicular to the missing rows (along the “ $2\sqrt{2}$ ” direction, see Fig. 2).

Surface	Calculated surface stress (N/m)	Calculated adsorbate-induced surface stress change (N/m)	Experimental adsorbate-induced surface stress change (N/m)
Cu(100)	1.89		
Cu(100)c(2×2)-O	-1.18	-3.07	-1.0
Cu(100)($\sqrt{2} \times 2\sqrt{2}$)R45°-O	-0.67/0.40	-2.56/-1.49	-0.6

The plots show that oxygen adsorption induces a compressive surface stress, i.e., the clean surface undergoes a curvature change towards a convex shape upon oxygen exposure. The oxygen-induced surface stress change saturates after an exposure of several hundred L, and it reaches a value of -1 N/m at 1000 L at 300 K, whereas exposure at 500 K induces a smaller stress change of -0.6 N/m. After termination of the exposure we again exposed the samples to oxygen, but no further change of either the stress or the diffraction pattern was observed. We therefore conclude that the results presented in Fig. 1 correspond to saturation coverages of oxygen. The small images show the resulting LEED patterns as measured in situ after oxygen exposure. These confirm the anticipated formation of a c(2×2) phase at 300 K and a ($\sqrt{2} \times 2\sqrt{2}$)R45° phase at 500 K.

Note that the initial oxygen-induced stress change as a function of exposure up to 60 L shows a similar steep gradient for exposures at both 300 K and 500 K, consistent with earlier evidence of the initial formation of the same overlayer phase at low coverages at the two different surface temperatures.¹³

The main conclusion of this stress measurement is that the formation of the oxygen-induced missing row reconstruction produces a smaller compressive stress change of -0.6 N/m, than that involved in the formation of the c(2×2) structure, which leads to a stress change of -1 N/m. We now consider the results of theoretical calculations of these same quantities.

III. COMPUTATIONAL DETAILS AND RESULTS

The DFT calculations reported here were conducted using the CASTEP computer code,¹⁹ (version 3.02) with the aid of the Cerius graphical interface.²⁰ The calculations were all conducted on 7-layer double-sided slabs with inversion symmetry around the central layer of atoms, with all layers allowed to relax perpendicular to the slab relative to this central layer. With both faces of the slabs having identical adsorbate coverage, the surface stress is the same on each face and is particularly trivial to extract from the calculated three-dimensional stress tensor. The surface stress was calculated analytically, based on the Hellmann-Feynman forces.

The lateral interatomic spacing within the slabs was fixed to the nearest neighbor value found in a similar DFT calculation for the bulk metal (using the same functionals and potentials); the associated bulk Cu lattice parameter was 3.600 Å.

All calculations were performed in the generalized gradient approximation (GGA) using PBE (Perdew, Burke, Ernzerhof) functionals²¹ with a 380 eV cut off energy. k -point sampling used the Monkhorst-Pack scheme with a constant k -point spacing of less than 0.025 Å⁻¹. This is a significantly smaller spacing (by about a factor of 2) than would typically be used in calculations performed for geometry or adsorption energy optimization, but we have found this finer sampling is essential for reasonable convergence of surface stress values which depend on energy and force gradients.²² For the (1×1), c(2×2), and ($\sqrt{2} \times 2\sqrt{2}$)R45° calculations the sampling grids were $16 \times 16 \times 2$, $12 \times 12 \times 2$, and $12 \times 6 \times 2$, respectively.

Table I summarizes the results of the present calculations of the absolute surface stress and adsorption-induced surface stress changes in these systems, and includes experimental values of these latter quantities. We should first remark on the values of the calculated surface stress for the clean surfaces for which the results of previous calculations have been published. For Cu(100), for which we report a value of 1.89 N/m, earlier calculations gave 1.38 N/m (Ref. 23) and 1.40 N/m (Ref. 24) in embedded-atom method calculations and 2.10 N/m (Ref. 25) from a DFT slab calculation. Clearly our values are in the general range of previous calculations. We should stress that as previously remarked both by us and other authors, the precision of surface stress calculations is generally much worse (probably no better than $\sim 10\%$, possibly worse) than in other quantities, such as adsorption energies and geometrical structural parameters, derived from total energy calculations. This is due to the extreme demands of adequate convergence and k -point sampling. Indeed, we note that we have also previously reported a value of 1.51 N/m for Cu(100) in our studies of related surface alloy systems.^{22,26} This value was also obtained from calculations on 7-layer metal slabs in GGA using PBE functionals, but the two calculations were based on different versions of the CASTEP code for which the available pseudopotentials were generated only in LDA and more recently, in GGA. This

TABLE II. Comparison of the structural parameters of the lowest energy surface structures found in this study with experimental measurements of the same quantities for O adsorption phases on Cu(100), the positions $1c$, $1s$, and the relaxations δy are defined in Fig. 2.

Surface	Parameter (all in Å)	Present DFT calculations	Experiment
Cu(100) $c(2 \times 2)$ -O	z_{O1}	0.68	0.52/0.73 (see text) (Ref. 12)
Cu(100)($\sqrt{2} \times 2\sqrt{2}$) $R45^\circ$ -O	z_{O1s}	0.31	0.17, [12] 0.10 (Refs. 8 and 9)
	z_{1c1s}	0.18	0.08, [12] -0.10 (Ref. 8), 0.05 (Ref. 9)
	δy_{1s}	0.19	0.29 (Ref. 12), 0.30 (Ref. 8), 0.10 (Ref. 9)
	δy_O	0.05	0.04 (Ref. 12), 0.00 (Ref. 8)
	z_{1s2}	1.90 (+7%)	1.88 (+4%) (Ref. 12), 2.04 (+13%) (Ref. 8), 2.06 (+14%) (Ref. 9)

difference in the combination of potential and approximation is known to lead to some differences in total energies²⁷ and also leads to a small difference in the bulk lattice parameter which may, at least in part, account for the different absolute surface stress value. A check on the surface stress of $c(2 \times 2)$ -Mn surface alloy phase on Cu(100) using the new pseudopotentials showed that the surface stress change was almost unchanged relative to the earlier result²⁶ obtained by the use of the different pseudopotentials.

The comparison of the calculated and experimental adsorption-induced surface stress changes given in Table I shows clear qualitative similarities, but significant disagreement in the absolute values. Specifically, both experimental and theoretical adsorbate-induced stress changes are compressive, and both show that this compressive change is very significantly smaller for the missing-row reconstruction than for the $c(2 \times 2)$ overlayer phase.

Before considering this comparison of theoretical and experimental surface stress changes in more detail, we remark briefly on the structural parameters obtained for the minimum energy $c(2 \times 2)$ and $(\sqrt{2} \times 2\sqrt{2})R45^\circ$ structural phases. These are summarized in Table II. Interlayer spacings are denoted z_{ab} where a and b define the layers, the adsorbate being represented by its elemental name while the substrate layers are numbered sequentially starting with 1 as the outermost layer; some additional identifiers are defined below. For the well-ordered Cu(100)($\sqrt{2} \times 2\sqrt{2}$) $R45^\circ$ -O surface, rather complete quantitative structure determinations are available from quantitative LEED (Refs. 8 and 9) and scanned-energy mode photoelectron diffraction (PhD) (Ref. 12) together with some information from surface x-ray diffraction.¹⁰ Figure 2 shows a schematic plan view of the structure and identifies some specific Cu atoms in the surface layer, notably those labeled s , adjacent to the steps at the edge of the missing rows and c , the center atoms midway between the missing rows. Figure 2 also identifies the parameters associated with the lateral relaxations alongside the missing rows. Table II includes the structural parameters obtained from the LEED and PhD studies, which show some significant quantitative variations, but very similar qualita-

tive trends. The DFT calculations yield values of the inter-layer spacings, top layer rumpling, and lateral relaxations, entirely consistent with these experimental trends. Notice, in particular, that the DFT calculations and all the experimental investigations show a significant relaxation of the Cu atoms adjacent to the missing row (δy_{1s}); this relaxation leads to an increase in all nearest-neighbor Cu-Cu distances within the surface layer, relative to those of the unreconstructed surface.

The state of experimental structural data for the $c(2 \times 2)$ phase is less clear. As discussed in the following section, this phase is commonly characterized by rather poor long-range order and a high density of antiphase domain boundaries, and can transform to the reconstructed phase with slight heating; although there are several early reports of the structural parameters that claim to be from the $c(2 \times 2)$ phase, these are not accompanied by clear evidence as to which surface phase was actually studied. However, a relatively

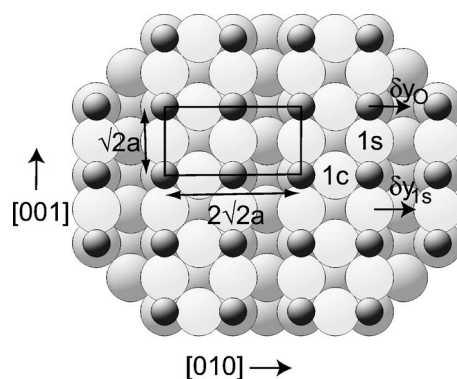


FIG. 2. Plan view of the Cu(100)($\sqrt{2} \times 2\sqrt{2}$) $R45^\circ$ -O surface structure showing the labelling of specific surface layer Cu atoms and the lateral displacement parameters appearing in Table II. The O atoms are shown as the smaller, darker shaded, spheres; the outermost layer Cu atoms are shown more lightly shaded than those of deeper layers. The rectangle shows the unit mesh dimensions in units of the Cu-Cu substrate interatomic spacing, a , while the two inequivalent $\langle 100 \rangle$ directions, $[010]$ and $[001]$ are labeled. The positions $1c$, $1s$, and relaxations δy , as used in Table II, are indicated.

recent PhD investigation of a low oxygen coverage phase at room temperature does provide an indication of the average O-Cu interlayer spacing.¹² Specifically, this experiment led to the suggestion that two different O-Cu layer spacings were involved, possibly associated with O atoms near the center at the edges of the small structural domains; these are the values reported in Table II, and they straddle the theoretical value. The overall conclusion to be drawn from Table II is thus that the DFT calculations do yield minimum energy structures for the two oxygen adsorption phases in good agreement with experiment.

IV. DISCUSSION

The results of the DFT calculations and the experiments (Table I) agree that oxygen adsorption on Cu(100) leads to a compressive change in the surface stress in both adsorption phases, and also agree that this compressive stress change is very significantly larger in the metastable $c(2 \times 2)$ overlayer phase than in the reconstructed $(\sqrt{2} \times 2\sqrt{2})R45^\circ$ phase. However, there are significant quantitative differences between the measured and calculated stress changes, and these differences may be significant in answering the question we originally posed, namely, could compressive stress relief be the (or a) driving force to the oxygen-induced missing row reconstruction? This is because the surface stress of the clean Cu(100) surface is known to be tensile, so a reduced compressive surface stress change on adsorption will only reduce the total energy if the absolute surface stress of the $c(2 \times 2)$ -O surface is, itself, compressive, and of larger absolute magnitude than that of the reconstructed phase. For surface stress change to drive the reconstruction it is the absolute value of the surface stress that must be reduced, and in this respect the experiments alone cannot answer this question, because they are only able to measure the stress change.

As may be seen from Table I, the DFT calculations clearly lead to a large absolute compressive surface stress for the $c(2 \times 2)$ phase, and a smaller absolute surface stress in the reconstructed $(\sqrt{2} \times 2\sqrt{2})R45^\circ$ phase. Interestingly, because of the anisotropy in the surface stress in this twofold symmetric reconstructed phase, the calculations find a compressive surface stress in the azimuthal direction parallel to the missing rows (the $\sqrt{2}$ direction) and a tensile surface stress perpendicular to the missing rows (the $2\sqrt{2}$ direction), but the absolute values of these surface stress tensor components are smaller than both the tensile surface stress of the clean surface and the compressive surface stress of the $c(2 \times 2)$ phase. The theoretical results do indicate, therefore, that the reconstruction does lead to a reduced *absolute* surface stress. Notice, though, that if one takes the (tensile) theoretical surface stress of the clean surface (+1.89 N/m) and the small compressive changes measured in the experiments following O exposure (-0.6 N/m and -1.0 N/m) then one would infer that the absolute surface stress remains tensile and is larger in the reconstructed phase, leading to the opposite conclusion regarding the role of surface stress change in the reconstruction. However, this comparison between the measured stress change and the calculated reference stress is not appropriate for the specific system investigated here as it neglects the

important role of local structural domains and their boundaries on the measured average stress, as discussed below.

In striving for a comparison between calculated and measured values we must consider the possible sources of error in both the calculations and the experiments. One potential source of reduced experimental values of adsorbate-induced surface stress changes is quite fundamental. In calculating the surface stress (in both theory and experiment) we assume that the surface is perfectly ordered over the whole crystal. In reality, an ordered adsorbate superstructure involves finite-sized domains on the surface; within these domains the adsorbate ordering may be of high quality, but between them will be narrow regions having poor order. Many of these regions will comprise antiphase domain boundaries, with associated discontinuities in the long-range ordering. Within these boundary regions one can expect local stress relief to occur, so the average surface stress over the whole crystal—the quantity measured experimentally—is expected to be less than the stress within a single ordered domain, which corresponds to the quantity calculated theoretically. Real surfaces also contain surface steps, and these can be another source of stress relief. In general, therefore, experimental measurements of surface stress changes are expected to yield values that are a lower limit of the true value for an ideally-ordered surface.

The general problem of domain effects is expected to be particularly serious for the Cu(100)/O experiments. STM data^{28,29} shows that the $c(2 \times 2)$ phase comprises very small domains and a high density of domain boundaries, so for this phase, in particular, stress relief at these boundaries could play a major role. In the case of the reconstructed $(\sqrt{2} \times 2\sqrt{2})R45^\circ$ phase, on the other hand, the long-range ordering is much better, but this phase has only twofold rotational symmetry, whereas the substrate has fourfold symmetry. The surface of a real crystal therefore comprises domains of two distinct rotational forms, related by a 90° azimuthal rotation; because these are equally probable, the resulting LEED pattern, an incoherent sum of the diffraction patterns from the different domains, shows the substrate fourfold symmetry, as seen in Fig. 1. This surface is therefore a case in which there is direct evidence of the presence of domain boundaries from the LEED pattern. The experimentally-measured surface stress change is thus isotropic, corresponding to the average of the anisotropic stress tensor components, but with the potential to be reduced from the average of the single-domain anisotropic stress by inter-domain stress relief. Overall, therefore, the fact that the experimental adsorbate-induced surface stress changes are of the same sign, but have a smaller magnitude than, the theoretically calculated ones, is consistent with the expected role of inter-domain stress relief in the experimental surfaces. We also note that these interdomain effects are likely to be more serious for the $c(2 \times 2)$ phase, so the qualitative experimental finding of a larger compressive stress change for this overlayer phase is likely to be reliable.

A further possible source of experimental error is the impact of any small adsorbate-precovage on the surface stress of the nominally clean Cu(100) surface. The experimental stress change measurements clearly show a rapid compressive

sive stress change (and thus a lowering of the tensile surface stress) in the earliest stages of oxygen dosing, so one may infer that if the starting surface was oxygen contaminated, the measured stress change would be much larger. Other adsorbates may also contribute to this effect. For example, Feibelman has calculated that a hydrogen coverage of 1 ML will reduce the tensile surface stress of Pt(111) from +6.27 N/m to +1.7 N/m, and on this same surface calculations indicated that oxygen lowered the surface tensile stress.³ Under these circumstances the reference state against which the stress change measurements are made would be one with a lower tensile surface stress than that of clean Cu(100). We note, however, that the initial rate of change of the measured surface stress with oxygen exposure at the two temperatures is the same, so we conclude that any possible initial surface contamination was the same for both temperatures, and thus the key experimental finding that the stress change is larger at 300 K is unaffected by this problem.

Of course, we should also consider possible errors in the theoretical values of the surface stress. Within a given computational approach (specifically the combination of functionals and approximation in a DFT calculation), the main source of error is incomplete convergence. As remarked earlier, the requirements for achieving this are significantly more demanding than those for obtaining good structural parameters, especially in requiring a much finer k -point sampling mesh, but our own previous tests indicate the calculations presented here should not have errors from this source of more than about 10%. The level of agreement in the absolute stress of the clean Cu(100) surface between calculations performed independently, which also introduces the effects of different methods of calculation, indicates an overall scatter of around 20%. There are rather few calculations of experimentally measured adsorbate-induced surface stress measurements with which to establish the general reliability of the methods beyond clean surfaces. Until very recently, there seem to have been only two such comparisons, those for the adsorption of oxygen on Pt(111),³ and of Mn on Cu(100) to form a surface alloy phase.²⁶ In both of these cases the experimental and theoretical results agree to within about 20%. Very recently, however, similar calculations of the O-induced compressive surface stress change on Ni(100) to form the $c(2 \times 2)$ phase have been reported³⁰ which yield values very significantly smaller than the experimentally measured values,^{2,4} a conclusion also found in our own recent DFT calculations.³¹ The limited evidence available therefore provides no reason to expect the present DFT calculations to seriously overestimate the compressive surface stress of the oxygen-covered Cu(100) surface phases.

Finally one might wonder why an 0.5 ML coverage of oxygen induces the missing row reconstruction of Cu(100), whereas the same adsorbate coverage leads to a $c(2 \times 2)$ surface structure on Ni(100). Presently our understanding of the interplay between adsorption and adsorbate-induced reconstruction is too limited to provide a simple explanation for this different behavior with respect to surface reconstruction, but it is now clear that Cu(100) and Ni(100) substrates do show pronounced differences in their behavior with respect to oxygen adsorption. In early literature there was considerable confusion as to whether or not the 0.5 ML coverage

phase of O on Cu(100) was a simple $c(2 \times 2)$ phase such as that seen for Ni(100)/O; early reports suggested this was the case, but subsequently some studies seemed to provide evidence that only the $(\sqrt{2} \times 2\sqrt{2})R45^\circ$ phase occurred.³² More recent STM studies,^{28,29} in particular, have shown rather clearly that such a phase can occur, but the adsorbate tends to form extremely small ordered islands with a very high density of antiphase domain boundaries, such that there may be little true long-range order; nevertheless, within the islands the local periodicity is $c(2 \times 2)$. The overall evidence is therefore that an unreconstructed $c(2 \times 2)$ overlayer phase of O on Cu(100) can exist, notably at around room temperature and below, but this appears to be only metastable and transforms to the missing-row $(\sqrt{2} \times 2\sqrt{2})R45^\circ$ phase with only modest annealing to ~ 100 – 200°C . The local unreconstructed oxygen overlayer also appears to be stable at low coverages, and there has been an experimental measurement of the local adsorption geometry.¹² Immediate creation of a well-ordered reconstructed $(\sqrt{2} \times 2\sqrt{2})R45^\circ$ phase occurs if the surface is exposed to oxygen at a similarly elevated temperature. These structural investigations indicate a higher propensity towards oxygen-induced surface reconstruction of Cu(100) in comparison to Ni(100).

V. CONCLUSIONS

The idea that relief of tensile surface stress plays an important role in driving the reconstruction of a small number of clean metal surfaces, most particularly Au(111), is well established.² In this case, the reconstructed surface layer has Au-Au nearest-neighbor distances smaller than those in the underlying bulk. By contrast, in the Ni(100)/C adsorption system, the clock reconstruction in the $(2 \times 2)p4g$ phase has increased Ni-Ni distances, which has been identified as resulting from the relief of the large compressive surface stress induced by the C adsorption. The Cu(100) $(\sqrt{2} \times 2\sqrt{2})R45^\circ$ -O missing-row reconstruction induced by O adsorption also involves a significant increase in nearest-neighbor Cu-Cu distances within the surface layer, though local relaxation adjacent to the missing rows, and is therefore a system in which one might expect that compressive stress relief could play a role. Our combined experimental and theoretical determinations of the surface stress in this surface phase, and in the metastable unreconstructed $c(2 \times 2)$ -O phase at the same nominal oxygen coverage appear to support this view. The oxygen adsorption does induce a compressive stress change in both adsorption phases, but this stress change is substantially larger in the unreconstructed phase, and the theoretical calculations indicate that in this phase the absolute surface stress is compressive and much larger in magnitude than that of the reconstructed surface. Our results therefore indicate that the missing row reconstruction provides an alternative mode of compressive stress relief to that of a clock reconstruction in an otherwise simple $c(2 \times 2)$ overlayer phase.

It is, of course, important to recognize that in any adsorbate-induced surface reconstruction many different factors contribute to the lowering of the total energy that causes the reconstruction to be favored. In a recent theoretical in-

vestigation of the Ni(100)/C adsorption system,^{30,33} in which there is a clear experimental correlation between the onset of the reconstruction and the change in surface stress,⁴ the effects of changes in the electronic structure were highlighted, and the authors actually concluded that their study “showed no direct link between surface reconstruction and surface stress.” Nevertheless, their calculations supported the experimental data that indicate that this reconstruction does lower the compressive surface stress, and as such the surface stress change must contribute to the lowering of energy. Our combined experimental and theoretical study of the Cu(100)/O system shows a similar correlation, and this cor-

relation can be related to the alternative mechanism of increasing the interatomic spacing of the metal atoms within the surface layer.

ACKNOWLEDGMENTS

M.J.H. acknowledges the support of the Physical Sciences and Engineering Research Council (U.K.). The majority of this work was performed on computing facilities provided by the Centre for Scientific Computing at the University of Warwick, with support from the Joint Research Equipment Initiative Grant No. JR00WASTEQ.

*Corresponding author.

Electronic address: d.p.woodruff@warwick.ac.uk

[†]Present address: Department of Physics, National Dong Hwa University, Hua-Lien 974, Taiwan.

¹*The Chemical Physics of Solid Surfaces vol. 7: Phase Transitions and Adsorbate Restructuring at Metal Surfaces*, edited by D. A. King and D. P. Woodruff (Elsevier, Amsterdam, 1994).

²H. Ibach, *Surf. Sci. Rep.* **29**, 193 (1997).

³P. J. Feibelman, *Phys. Rev. B* **56**, 2175 (1997).

⁴D. Sander, U. Linke, and H. Ibach, *Surf. Sci.* **272**, 318 (1992).

⁵J. H. Onuferko, D. P. Woodruff, and B. W. Holland, *Surf. Sci.* **87**, 357 (1979).

⁶Y. Gauthier, R. Baudoing-Savois, K. Heinz, and H. Landskron, *Surf. Sci.* **251**, 493 (1991).

⁷R. Terborg, J. T. Hoefl, M. Polcik, R. Lindsay, O. Schaff, A. M. Bradshaw, R. L. Toomes, N. A. Booth, D. P. Woodruff, E. Rotenberg, and J. Denlinger, *Surf. Sci.* **446**, 301 (2000).

⁸H. C. Zeng, R. A. McFarlane, and K. A. R. Mitchell, *Surf. Sci.* **208**, L571 (1998).

⁹A. Atrie, U. Bardi, G. Casalone, G. Rovida, and E. Zanazzi, *Vacuum* **41**, 333 (1990).

¹⁰I. K. Robinson, E. Vlieg, and S. Ferrer, *Phys. Rev. B* **42**, 6954 (1990).

¹¹M. C. Asensio, M. J. Ashwin, A. L. D. Kilcoyne, D. P. Woodruff, A. W. Robinson, Th. Lindner, J. S. Somers, D. E. Ricken, and A. M. Bradshaw, *Surf. Sci.* **126**, 1 (1990).

¹²M. Kittel, M. Polcik, R. Terborg, J. T. Hoefl, P. Baumgärtel, A. M. Bradshaw, R. L. Toomes, J.-H. Kang, D. P. Woodruff, M. Pascal, C. L. A. Lamont, and E. Rotenberg, *Surf. Sci.* **470**, 311 (2001).

¹³M. Wuttig, R. Franchy, and H. Ibach, *Surf. Sci.* **213**, 103 (1989).

¹⁴K. W. Jacobsen and J. K. Nørskov, *Phys. Rev. Lett.* **65**, 1788 (1990).

¹⁵E. A. Colbourn and J. E. Inglesfield, *Phys. Rev. Lett.* **66**, 2006 (1991); I. Merrick, J. E. Inglesfield, and H. Ishida, *Surf. Sci.*

551, 158 (2004).

¹⁶S. Stolbov and T. S. Rahman, *Phys. Rev. Lett.* **89**, 116101 (2002); S. Stolbov, A. Kara, and T. S. Rahman, *Phys. Rev. B* **66**, 245405 (2002).

¹⁷D. Sander, S. Ouazi, A. Enders, Th. Gutjahr-Löser, V. S. Stepanyuk, D. I. Bazhanov, and J. Kirschner, *J. Phys.: Condens. Matter* **14**, 4165 (2002).

¹⁸ $1/R_1 = 6(\tau_1 - \nu\tau_2)/Yr^2$; see: D. Sander, A. Enders, and J. Kirschner, *Europhys. Lett.* **45**, 208 (1999).

¹⁹M. C. Payne, M. P. Teter, D. C. Allen, T. A. Arias, and J. D. Joannopoulos, *Rev. Mod. Phys.* **64**, 1045 (1992).

²⁰<http://www.accelrys.com/ceirus2/qmw.html>

²¹J. P. Perdew, K. Burke, and M. Ernzerhof, *Phys. Rev. Lett.* **77**, 3865 (1996).

²²M. J. Harrison, D. P. Woodruff, and J. Robinson, *Surf. Sci.* **572**, 309 (2004).

²³P. Gumbsch and M. S. Daw, *Phys. Rev. B* **44**, 3934 (1991).

²⁴J. Wan, Y. L. Fan, D. W. Gong, S. G. Shen, and X. Q. Fan, *Modell. Simul. Mater. Sci. Eng.* **7**, 189 (1999).

²⁵Y. Yoshimoto and S. Tsuneyuki, *Appl. Surf. Sci.* **237**, 274 (2004).

²⁶M. J. Harrison, D. P. Woodruff, and J. Robinson, *Phys. Rev. B* **72**, 113408 (2005).

²⁷M. Fuchs, M. Bockstedte, E. Pehlke, and M. Scheffler, *Phys. Rev. B* **57**, 2134 (1998).

²⁸K. Tanaka, T. Fujita, and Y. Okawa, *Surf. Sci.* **410**, L407 (1998).

²⁹T. Fujita, Y. Okawa, Y. Matsumoto, and K. I. Tanaka, *Phys. Rev. B* **54**, 2167 (1996).

³⁰S. Hong, A. Kara, T. S. Rahman, R. Heid, and K. P. Bohnen, *Phys. Rev. B* **69**, 195403 (2004).

³¹M. J. Harrison, D. P. Woodruff, and J. Robinson (to be published).

³²R. Mayer, C.-S. Zhang, and K. G. Lynn, *Phys. Rev. B* **33**, 8899 (1986).

³³S. Stolbov, S. Hong, A. Kara, and T. S. Rahman, *Phys. Rev. B* **72**, 155423 (2005).